

NUMERICAL SIMULATION STUDY ON THE INFLUENCE OF WING SPACING OF DRAGONFLY-INSPIRED FLAPPING WINGS

Yang Luo^{1,2}, Lei Wang^{1,2}, Jiaxin Wang^{1,2}, Xinyu Lang^{1,2}& Xiaojun Yang^{1,2,3}

¹School of Aeronautics, Northwestern Polytechnical University, Xi'an, Shaanxi 710072, China
²National Key Laboratory of Aircraft Configuration Design, Xi'an, Shaanxi 710072, China
³Research & Development Institute of Northwestern Polytechnical University in Shenzhen, Shenzhen, Guangdong, 518057, China

Abstract

Dragonflies are widely concerned because of their superb flying skills, which have unique tandem wings. The tandem wings can make full use of the interference of various spatial vortices to obtain efficient flight capability. Because of the variety of dragonflies, the wing distribution between tandem wings is also different. In this paper, the aerodynamic performance of the dragonfly-inspired tandem wings is analyzed using the Computational Fluid Dynamics (CFD) method considering the wing spacing between tandem wings. The force coefficient and vortex structure in forward flight are analyzed. The results show that variation of the spacing will affect the time when the vortex of the forewing (FW) reaches the hindwing (HW), resulting in the lag of the peak and trough of the force coefficient curve of HW. The aerodynamic performance of HW can be improved by properly adjusting the distance between FW and HW. The conclusion can provide theoretical guidance for the design of the dragonfly-inspired tandem flapping wing aircraft.

Keywords: Dragonfly flight, Tandem wings, Wing spacing, Aerodynamics, Forward flight

1. Introduction

The dragonfly can perform various flight maneuvers with high performance, such as forward flight, backward flight, hovering, maneuvering flight, and so on.[1] The dragonfly has unique tandem wings, which can effectively use a variety of unsteady airflow interference to achieve efficient aerodynamic performance through complex motion parameter interaction. In its flight process, the interaction between tandem wings is the main source of producing larger thrust, lift, and stronger maneuverability.

In order to reveal the influence of the interference between forewing (FW) and hindwing (HW) on the aerodynamic performance of the dragonfly, lots of simulation and observation experiments have been done. Bode-Oke et al [2] found that the combination of the attack angle and velocity results in significant aerodynamic force. Shumway et al [3] studied the wing deformation of the dragonfly and found that the average lift and thrust caused are small by the wing deformation. Hefler et al [4] discovered varying effects of the vortex produced along different areas of the HW. Swain et al [5] investigated the temporal effects of the wake capture and dipole structure by analyzing 2D vorticity flow fields surrounding the fore and hind wings. Rüppell et al [6] analyzed the flight of dragonflies by shooting in slow motion, and observed that the phase difference will gradually change when flying slowly. Shanmugam et al [7] have studied the influence of the phase difference and distance between the FW and HW. The study revealed that both factors influence the aerodynamic interference of the tandem wings. Zou et al [8] found that the interactions between FW and HW greatly affect their vortex structure and flight performance.

There are about 6,000 named species of Odonata in the world, and each family has obvious biological differences[9]. So it is speculated that the wing spacing of the dragonfly will affect its aerodynamic performance. Some researchers also pay attention to the distance of tandem wings. Wu Qi Gong et al[10] studied the phase difference and wing spacing of tandem wings, and found that the increase in the mean thrust coefficient of the FW is caused by the leading edge vortex (LEV) and stagnation region of the HW. K. B. Lua et al[11] used experimental and numerical methods to study the aerodynamic performance of the phase difference and wing spacing at Reynolds number of 5000. Results show that increasing wing spacing has a similar effect as reducing the phase angle.

Abdelhakim Younsi et al[12] observed the effects of the asymmetry in flapping duration, wing spacing, and phase difference on the aerodynamic performance of tandem wings. The three values when the propulsion efficiency is optimal are obtained. Zhaokai Lu[13] carried out a three-dimensional numerical simulation analysis on a set of NACA0011 arranged in tandem configuration. The results show that as the distance decreases, the lift of the FW increases sharply, and the lift of the HW decreases, but the total lift remains unchanged.

However, the research on the wing spacing of tandem wings is under the condition of two-dimensional calculation, and the wings of the FW and HW are the same. In order to clarify the influence of wing spacing, a calculation model is established by using real dragonflies. Taking the horizontal distance and vertical distance between the HW and the FW as the main research parameters. The influence of the change of wing spacing on the aerodynamic performance of the FW and HW is analyzed by Computational Fluid Dynamics (CFD). It is hoped that the research results can provide the theoretical basis for the research of dragonfly-inspired flapping-wing aircraft.

2. Materials and Methods

2.1 Tandem Wings model

In order to figure out the influence of wing spacing on the aerodynamic characteristics of dragonfly tandem wings, the real dragonfly wing is used as a reference to establish the tandem wings model (as shown in Figure 1) and flapping kinematics for the numerical simulation. In Figure 1, b_f is the semi-span of the FW, and b_h is the semi-span of the HW. The I indicates the distance between tandem wings and the symmetry plane. Detailed geometric data of the tandem wings model are provided in Table 1.

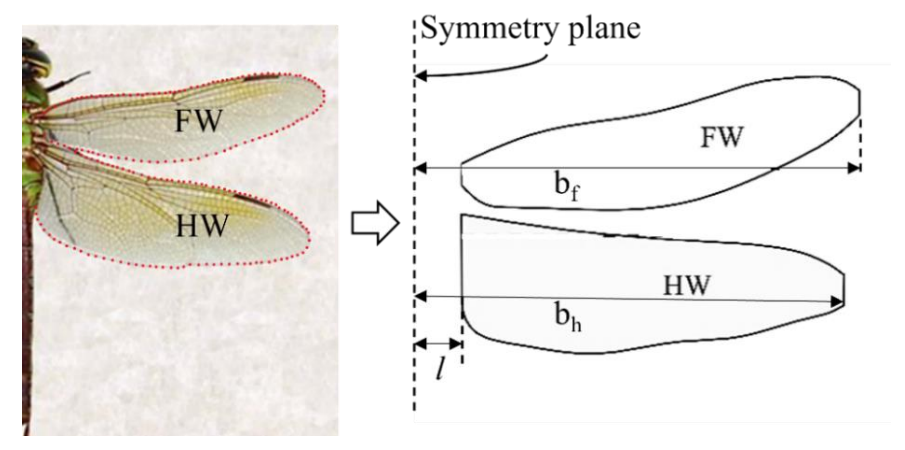


Figure 1 – The tandem wings model.

Because of the uneven variation of the chord length of real dragonfly wings, the mean chord length is taken as the chord length of the FW and HW. The distance from the quarter chord length of the FW to the quarter chord length of the HW is 5.93×10^{-3} m.

Table 1 – Wing parameters.				
Parameter	Value			
Mean chord length of FW (c_f)	8.67×10^{-3} m			
Mean chord length of HW (c_h)	1.15×10^{-2} m			
Semi-span of FW (b_f)	4.7×10^{-2} m			
Semi-span of HW (b _h)	4.5×10^{-2} m			
Distance between the wing heel and the symmetry plane(I)	8.67×10^{-3} m			
Wing thickness(d)	8.6×10^{-5} m			

2.2 Motion kinematics

The movements of the tandem wings combined with flapping and pitching motion are described in Figure 2. The flapping motion axis in the XOZ plane. The pitching motion rotates around an axis, which is positioned a quarter of the chord length of the FW and HW. The stroke plane angle is

defined as β .

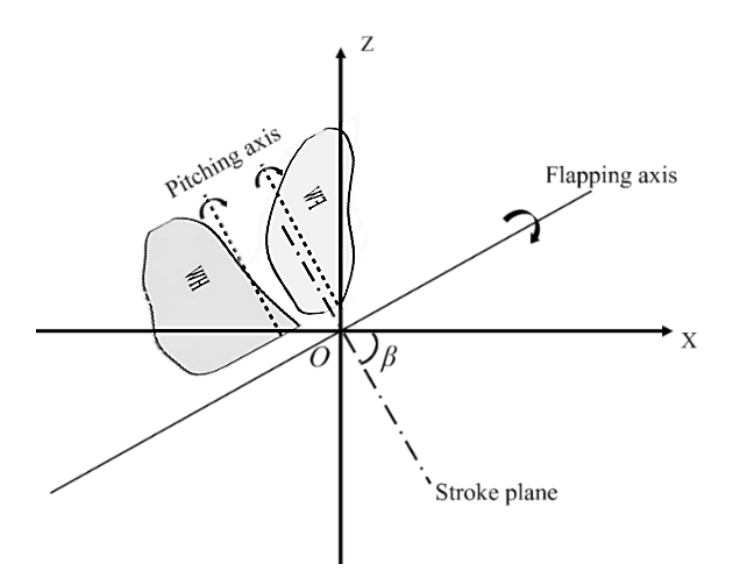


Figure 2 – Motion model.

The governing equations of flapping and pitching motion are given as follows.

$$\phi_{FW}(t) = \phi_m \sin(2\pi f t) \tag{1}$$

$$\alpha_{FW}(t) = \alpha_m \sin(2\pi f t + \varphi) \tag{2}$$

$$\phi_{HW}(t) = \phi_m \sin(2\pi f t + \psi) \tag{3}$$

$$\alpha_{HW}(t) = \alpha_m \sin(2\pi f t + \psi + \varphi) \tag{4}$$

where Φ_m and α_m is the amplitude of the flapping and pitching and set to 30°. f is the flapping frequency. ϕ is the phase angle between the flapping and pitching motion, and ψ is the phase difference between the FW and HW. In order to ensure the efficient flight of tandem wings, the phase angle between the flapping and pitching motion needs to be kept at 90 degree [14]. Some motion parameters during calculation are shown in Table 2.

Table 2 – Motion parameters.

Name	parameter
Re	1286
Velocity (u)	2.2m/s
Flapping frequency (f)	30Hz
Phase difference (ψ)	90 degree
Stroke plane angle (β)	75 degree

The main variable parameter in this study is the wing spacing, and the wing spacing is defined by controlling the horizontal and vertical distance between the HW and the FW. The wing spacing is shown in Table 3.

Table 3 – Define the wing spacing.

	The distance between the HW and the FW		
Horizontal distance (x-axis)	h₀(initial distance)	h ₀ +2c	h ₀ +4c
Vertical distance (z-axis)	I_0 (initial distance)	<i>l</i> ₀ +2 <i>c</i>	<i>I</i> ₀ +4c

The quarter chord distance between the FW and the HW is defined as the initial distance. Where $c=1/2*(c_f+c_h)$. The force on the stroke plane is divided into vertical force (F_V) and horizontal force (F_H). The force is defined as shown in Figure 3. The time-averaged force coefficients can be obtained as shown in equations 5 and 6 respectively.

$$\overline{C_V} = \frac{1}{T} \int_t^{t+T} \frac{F_V}{\frac{1}{2} \rho \mathbf{u}^2 S} dt$$
 (5)

$$\overline{C_H} = \frac{1}{T} \int_t^{t+T} \frac{F_H}{\frac{1}{2} \rho \mathbf{u}^2 S} dt \tag{6}$$

Where T is the flapping period.

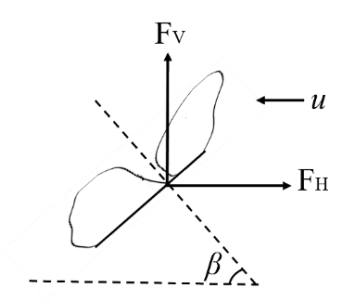


Figure 3 – Force definition.

2.3 Computational conditions

The transient simulations are investigated numerically using the computational fluid dynamics software by solving the Navier–Strokes equations. The equations governing the flow in the numerical solver were the transient and incompressible continuity equation and the Navier-Stokes equation. For all the cases in this study, the laminar model is used to stimulate. Momentum, turbulent kinematic energy, and specific dissipation rate are discretized with a second-order upwind scheme. Second-order accuracy is applied to calculate the pressure. Transient Formulation is First Order Implicit. A coupled algorithm is employed for the pressure-velocity coupling.

The motions of the flapping wings are simulated based on an overset mesh technique. The overset mesh consists of a background mesh and a component mesh. In the process of dynamic movement, the background mesh remains static, while the entire component mesh moves as a rigid body. The component mesh utilizes unstructured grids, and the wing surface generates structured grids. The assembled mesh is shown in Figure 4 (a), and the grid area is a cube of $120c_i \times 120c_i \times 100c_i$. The component mesh is composed of a cylinder with a radius of $10c_i$ and $10c_i$, as shown in Figure 4 (b). The wing surface mesh is shown in Figure 4 (c). The height of the first grid of the boundary layer is 0.08mm to ensure Y⁺=1.

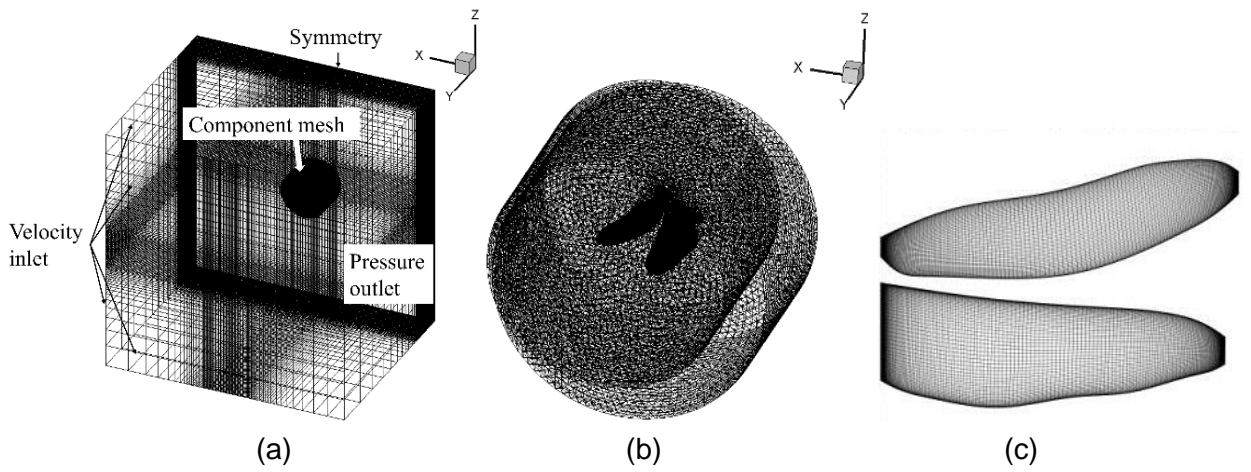


Figure 4 – Computational domain setup for the tandem wings(a) Assembled mesh; (b) Component mesh;(c) Wing surface mesh.

2.4 Solver validation

According to the experiment of S. Heathcote [15] in 2006, the method is verified. The model used in this experiment is NACA0012, with a chord length(c_0) of 100mm, and a spanwise length of 600mm. The wing motion is defined as follows:

$$s = 0.175c_0 \cos(2\pi ft) \tag{7}$$

Where s is the displacement of the wing root and f is the oscillating frequency. The Reynolds number is defined as $Re = U_{\infty}c/v$, where v is the dynamic viscosity of water and $U_{\infty} = 0.939m/s$ is the freestream velocity. Based on the conditions, the results are compared with the calculation results of Liu [16]. As shown in Figure 5, the agreement is generally good for the parameters, with a small discrepancy appearing at the peak and valley values. It should be noted that the experimental data measured from the inflexible wing still shows small flexibility rather than a fully rigid wing. This might be responsible for a slight thrust force increase and phase delay. According to the comparison results, the overset method is feasible.

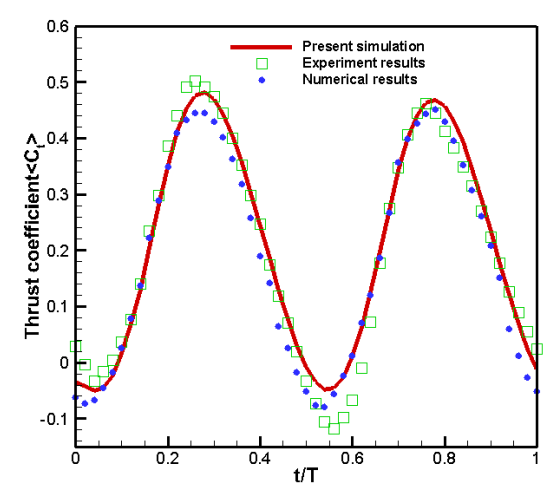


Figure 5 – Comparison of experiment and CFD simulations.

3. Results and discussion

3.1 Aerodynamic forces

In this simulation, nine different cases were calculated to study the influence of the wing spacing between the FW and HW on the forward flight. All cases were calculated for three periods and the results of the last period are analyzed. Figure 6 shows the force coefficient of the FW in different wing spacing. The gray area represents the flapping downstroke, and the light zone indicates the wing is flapping upstroke. A variety of curve styles means a change in horizontal distance. Distinguish the vertical distance from the HW to the FW with colors. The name of the curve is followed by the time-averaged force coefficient. In Figure 6, at the time of t/T=0.55, the force coefficient curves all showed small fluctuations. At other times, the force coefficient curve changes consistently. The change of wing spacing had little influence on the force coefficient of the FW.

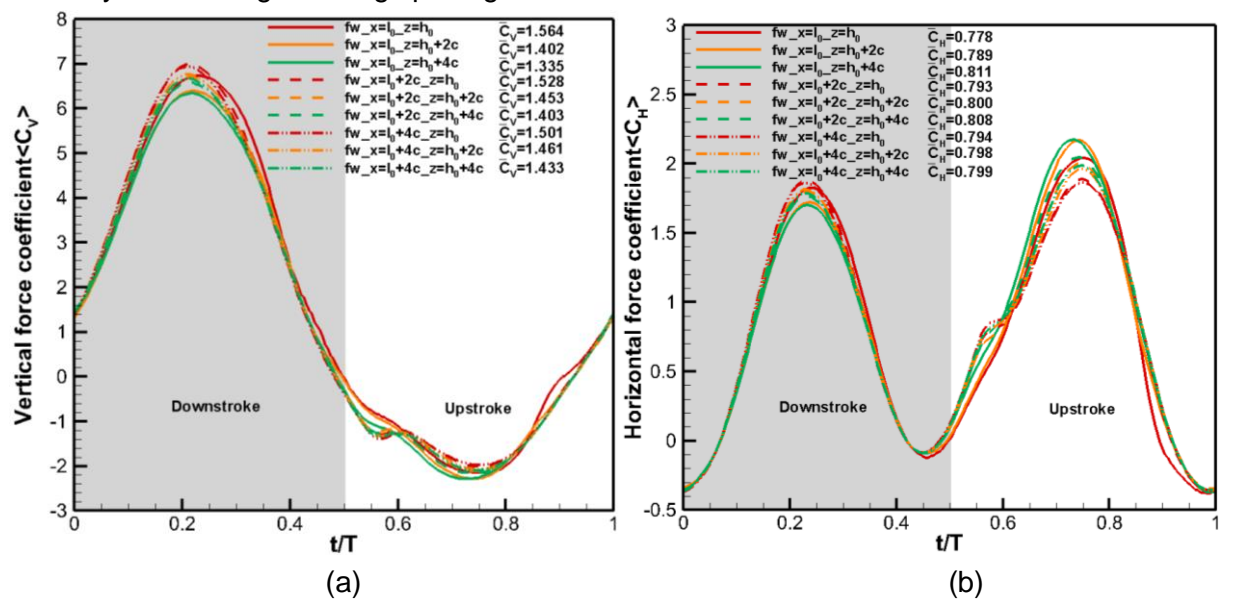


Figure 6 – The force coefficient of FW under different wing spacing. (a) Vertical force coefficient; (b) Horizontal force coefficient.

As can be seen from Figure 7, the force coefficient curve of the HW is different. Because there is 90 degree phase difference between the FW and the HW, the force coefficient curve of the HW is shifted forward by a quarter period. At the trough of the vertical force coefficient and the peak of the horizontal force coefficient, the curve has a more chaotic change. The curve at the complex change is enlarged to the left. In order to clarify the influence at different positions, the curves at typical positions are selected for thickening.

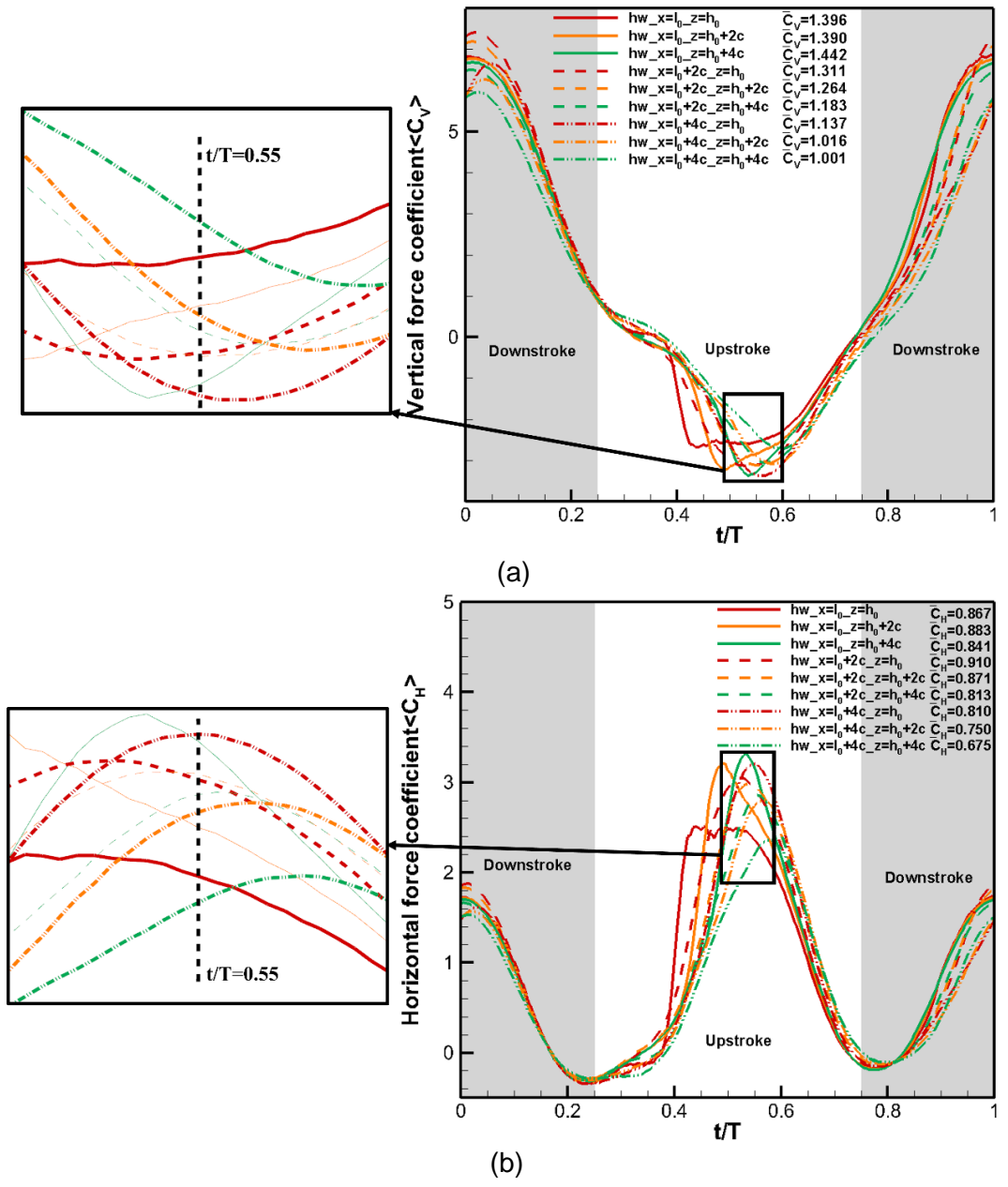


Figure 7 – The force coefficient of HW under different wing spacing. (a) Vertical force coefficient; (b) Horizontal force coefficient.

In Figure 7(a), it is found that the value trough becomes smaller and smaller and the time of the trough appears gradually lags behind, with the increase of the vertical distance. The change in the red curve also shows the same phenomenon. With the increase of the horizontal distance, the value of the vertical force coefficient of the HW also decreases, and the trough also lags behind. The change of the dashed line of the vertical force coefficient also appears obvious lag phenomenon, but there is only a slight increase in the value of the trough. Interestingly, when the horizontal distance is h_0+4c , increasing the vertical distance still has a trough lag phenomenon. However, the value of the trough is gradually increasing. The change of the green curve shows that when the vertical distance is l_0+4c , increasing the horizontal distance will also lead to the gradual increase of the trough value.

A similar phenomenon occurs in the horizontal force coefficient shown in Figure 7(b). The difference

is that the curve variation law is opposite to the vertical force coefficient. The change in trough value is more obvious when the horizontal distance is h_0 +2c. When the spacing changes at the initial horizontal position or the initial vertical position, the vertical force coefficient decreases and the horizontal force coefficient increases gradually with the increase of the spacing. As the horizontal or vertical spacing increases by 2c or more, the vertical force coefficient begins to increase, and the horizontal force coefficient gradually decreases. This shows that the change of spacing in different directions has little influence, but the change of spacing has a great influence on the aerodynamic force on the HW. In order to clear the influence of the vortex during the flapping upstroke, five typical wing spacing at t/T=0.55 are selected for fluid-structure analysis.

3.2 Fluid structures

Figure 8 shows five pressure coefficient contours of different wing spacing at the moment of HW mid-upstroke (t/T=0.55). The pressure coefficient (cp) is defined by equation 8, and the range of the cp in all examples is -1 to 4.

$$cp = \frac{pressure}{\frac{1}{2}\rho u^2} \tag{8}$$

At t/T=0.55, it can be clearly seen that there is a high-pressure zone on the upper surface of the HW near the leading edge of the wing tip. With the increase of horizontal distance, the high-pressure area at the tip is gradually increasing. Meanwhile, the low-pressure area at the root of the HW also increases. When the horizontal spacing is kept at *l*₀+4c, with the increasing of the vertical distance, the high-pressure zone is not obviously affected. However, the low-pressure zone at the wing root is still expanding. This explains the phenomenon that the trough values of the force coefficient curve change inversely after increasing the spacing in different directions.

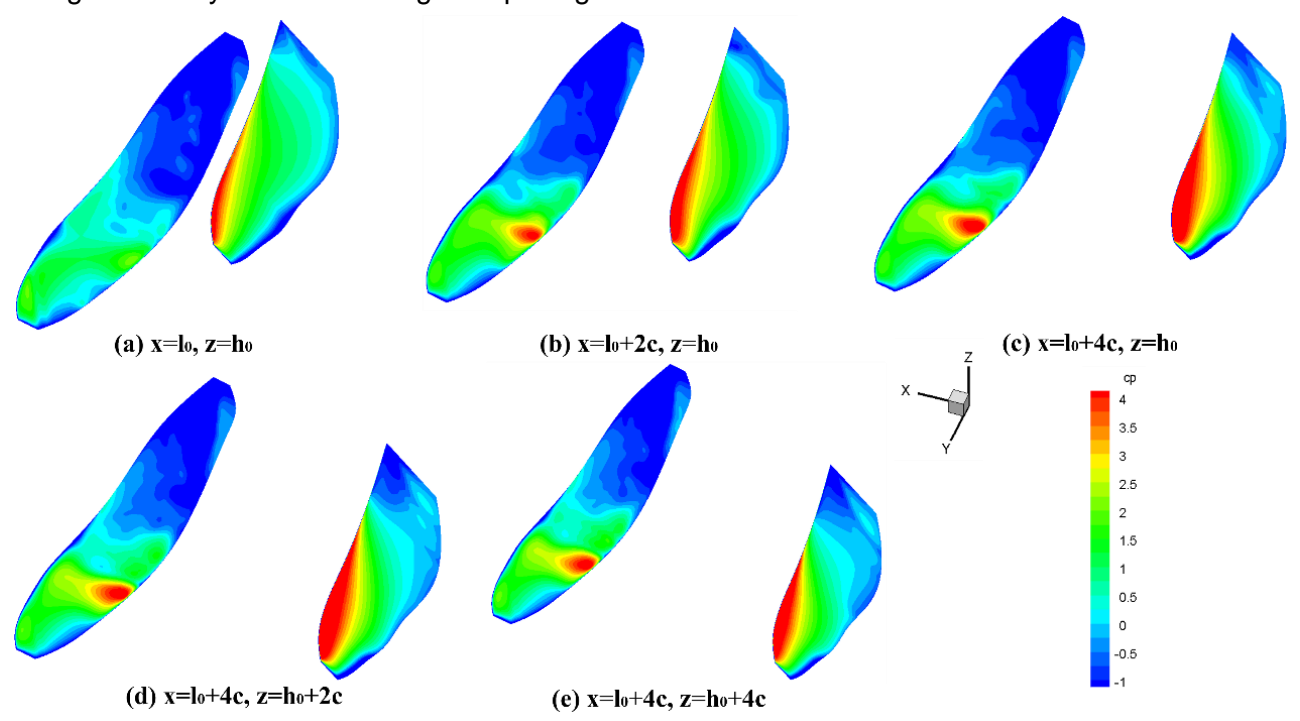


Figure 8 – Pressure coefficient contour of different wing spacing at the moment of HW mid-upstroke (t/T=0.55).

In order to explore the causes of the pressure change on the HW surface, the wing root and the wing tip vortex section are selected for observation. Figure 9 presents the vortex contour within the slice at t/T=0.55. The first line shows the vortex at the wing root and the second line shows the vortex at the wing tip.

At the wing root, when the vertical spacing is constant and the horizontal spacing is increased, the HW gradually moves away from the influence zone of the trailing edge vortex(TEV) of the FW. The vortex absorbed by the lower surface of the HW gradually decreases, so the low-pressure area at

the HW root expands. With the magnification of vertical spacing, the HW is completely separated from the vortex zone of the FW, which leads to the continuous expansion of the low-pressure zone of the HW root.

In Figure 9(a), at the wing root, the leading edge vortex(LEV) of the FW is cut off by the HW. Then, the LEV of the FW affects the vortex on the upper surface of the HW. And only a small part of the LEV is absorbed by the lower surface of the HW. With the expansion of horizontal spacing, the LEV intercepted by the HW is reduced. The influence of the LEV on the lower surface of the HW increases gradually, which leads to the expansion of the high-pressure zone at the HW tip. With the increase of vertical spacing, the high-pressure area at the wing tip does not expand further, because the HW has absorbed part of the LEV of the FW and left the vortex zone at this time.

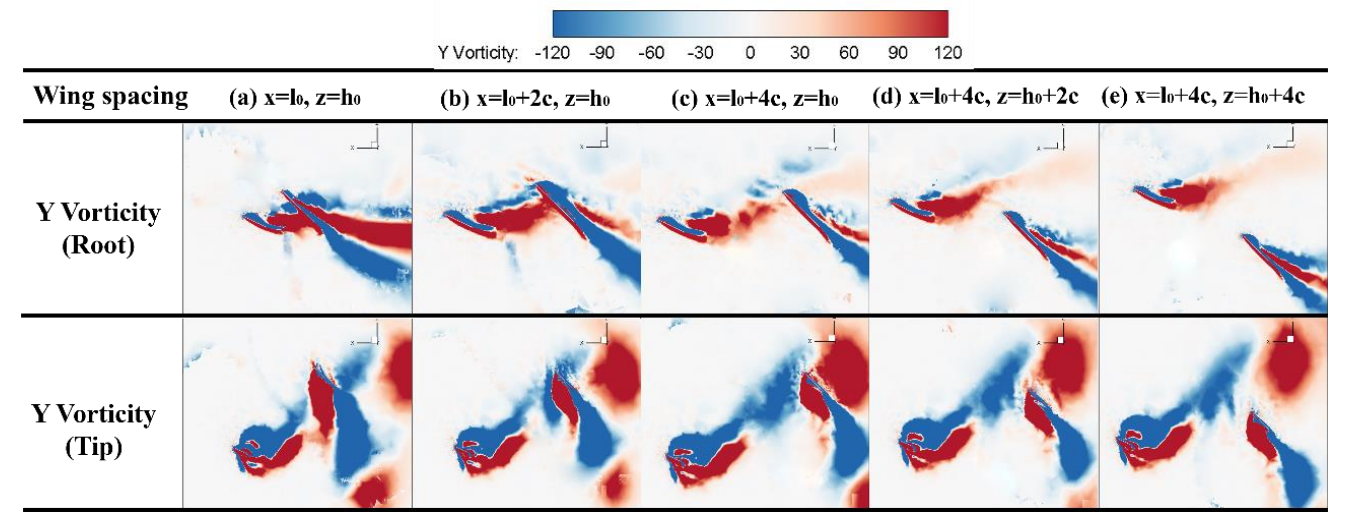


Figure 9 – Vortex contour within the slice at the wing root and wing tip at the moment of HW midupstroke (t/T=0.55).

The wing spacing between the FW and HW has impacts on the aerodynamic force of tandem configuration. The wing spacing not only affects the time when the vortex generated by the FW reaches the HW, but also has different effects at the root and tip of the HW. The vortex capture of the HW can be adjusted by changing the wing spacing between the FW and the HW properly. Meanwhile, the aerodynamic characteristics of the HW can be changed to make the HW have good aerodynamic performance.

4. Conclusions

In this paper, the aerodynamic characteristics of the tandem wings have been assessed based on the overset mesh technique. Several wing spacing are investigated to evaluate the effects of different spacing between the FW and HW on the aerodynamic performance of the tandem wings. The conclusions are as follows:

- (1) The influence of spacing change in different directions is similar. The main influence on the aerodynamic performance of the HW is the change of spacing. The change of the spacing will affect the time when the vortex of the FW reaches the HW, resulting in the lag of the peak and trough of the force coefficient curve during the flapping of the HW.
- (2) The increase of the HW spacing within 2c will raise the peak value of the horizontal force coefficient of the HW. When the range is greater than 2c, the peak value of the horizontal force coefficient will decrease. Thus, it is beneficial to improve the aerodynamic performance of the HW by properly adjusting the distance between the FW and the HW within I₀+2c or h₀+2c.

5. Contact Author Email Address

The contact author email address: xjyang518@nwpu.edu.cn

6. Acknowledgments

This work is financially supported by the Shenzhen Science and Technology Program and Research under Grant No. JCYJ20220530161808018, and Guangdong Basic and Applied Basic Research

INSERT RUNNING TITLE HERE

Foundation under Grant No. 2023A1515010776. Key R&D Program in Shaanxi Province of China under Grant No. 2023-YBGY-372.

7. Copyright Statement

The authors confirm that they, and/or their company or organization, hold copyright on all of the original material included in this paper. The authors also confirm that they have obtained permission, from the copyright holder of any third party material included in this paper, to publish it as part of their paper. The authors confirm that they give permission, or have obtained permission from the copyright holder of this paper, for the publication and distribution of this paper as part of the ICAS proceedings or as individual off-prints from the proceedings.

References

- [1] Wootton R, "Dragonfly flight: morphology, performance and behavior," International Journal of Odonatology 23, (2020).
- [2]. A.T. Bode-Oke, S. Zeyghami, H. Dong, "Flying in reverse: kinematics and aerodynamics of a dragonfly in backward free flight," J. R. Soc. Interface 15(143), 20180102 (2018).
- [3]. N. Shumway, M. Gabryszuk & S. Laurence, "The impact of dragonfly wing deformations on aerodynamic performance during forward flight," Bioinspir. Biomim 15, 026005 (2020).
- [4]. Hefler C, Qiu H, Shyy W, "Aerodynamic characteristics along the wing span of a dragonfly Pantala flavescens," Journal of Experimental Biology 221(19), (2018).
- [5]. Swain P K, Dora S P, "Experimental and numerical investigation of wing—wing interaction and its effect on aerodynamic force of a robotic dragonfly during hovering and forward flight," Archive of Applied Mechanics 91(5), (2021).
- [6]. Rüppell G, Hilfert-Rüppell D, "Rapid acceleration in Odonata flight: highly inclined and in-phase wing beating," International Journal of Odonatology 23(1), (2020).
- [7]. Shanmugam A R, Sohn C H, "Numerical investigation of the aerodynamic benefits of wing-wing interactions in a dragonfly-like flapping wing," Journal of Mechanical Science and Technology 33, (2019).
- [8]. Zou P Y, Lai Y H, Yang J T, "Effects of phase lag on the hovering flight of damselfly and dragonfly," Physical Review E 100(6), (2019).
- [9] Silsby J, "Dragonflies of the World," CSIRO publishing, (2001).
- [10] Gong W Q, Jia B B, "Experimental study on mean thrust of two plunging wings in tandem," AIAA Journal 53(6), (2015).
- [11] Lua K B, Lu H, Zhang X H, et al, "Aerodynamics of two-dimensional flapping wings in tandem configuration," Physics of Fluids 28(12), (2016).
- [12] Younsi A, El-Hadj A A, Abd Rahim S Z, et al, "Effects of the wing spacing, phase difference, and downstroke ratio on flapping tandem wings," Proceedings of the Institution of Mechanical Engineers, Part C: Journal of Mechanical Engineering Science 236(9), (2022).
- [13] Lu Z, "Numerical Analysis of Lift and Drag Characteristics of NACA0011 Airfoils in Tandem Configuration," International Conference on Mechanical, Aerospace and Automotive Engineering, (2021).
- [14]. Azuma A, Azuma S, Watanabe I, et al, "Flight mechanics of a dragonfly," Journal of experimental biology 116(1), (1985).
- [15]. Heathcote S, Wang Z, Gursul I, "Effect of spanwise flexibility on flapping wing propulsion," Journal of Fluids and Structures 24(2), (2008).
- [16]. Liu H, "Integrated modeling of insect flight: from morphology, kinematics to aerodynamics," Journal of Computational Physics 228(2), (2009).